RESEARCH ARTICLE

WILEY

CircRNA_0008194 functions as a ceRNA to promote invasion of hepatocellular carcinoma via inhibiting miR-190a/AHNAK signaling pathway

Wei Liu[1,2] | Ying Pan[2] | Hengbo Zhu[2] | Yi Zhou[2] | Hui Zhang[2] | Liu Liu[2] | Qing Liu[2] | Guozhong Ji[1]

[1]Medical Center for Digestive Diseases, The Second Affiliated Hospital of Nanjing Medical University, Nanjing, China

[2]Medical Center for Digestive Diseases, The Fourth Affiliated Hospital of Nanjing Medical University, Nanjing, China

Correspondence
Guozhong Ji, Medical Center for Digestive Diseases, the Second Affiliated Hospital of Nanjing Medical University, Jiangjiayuan 121#, Nanjing, Jiangsu Province 210000, China.
Email: jnjmu2021@163.com

Abstract

Background: Hepatitis B virus infection was identified as the main risk factor of hepatocellular carcinoma (HCC) in China, which induced a high morbidity and mortality. In recent years, circRNAs were reported involving in the oncogenesis and development of multiple malignant tumors.

Method: Bioinformatical analysis has been employed to predict the relevant circRNA with AHNAK. The loss of function and gain of function have been used by knocking-down circRNA through the shRNA technology while overexpressing through lentivirus infection. Dual-luciferase reporter assay was used to detect circRNA binding to miRNA and target genes. We further used immunoprecipitation technique to detect the binding ability between non-coding RNAs.

Results: In this study, according to the previous report, we mainly focused on AHNAK, which has been confirmed as an oncogene involving in the metastasis of HCC. Bioinformatics analysis showed that circ_0008194 could be spliced by AHNAK. In this study, the abnormal upregulated circ_0008194 in tumor tissues was detected. The positive correlation between circ_0008194 and AHNAK was also confirmed. Through knockdown and overexpression of circ_0008194, we conducted in vitro functional studies. We found circ_0008194 could induce the invasion of cells in vitro. Mechanically, circ_0008194 presented the binding ability with miR-190a causing the suppression of miR-190a expression, causing the competitive inhibition of AHNAK, resulting in the promotion of EMT.

Conclusion: Our results suggested that circ_0008194 may act as a sponge to adsorb miR-190a, thereby promoting the expression of AHNAK and promoting the metastasis of liver cancer tumors.

KEYWORDS
ceRNA, circRNA, HCC, invasion, metastasis

---

1 | INTRODUCTION

As a common abdominal cancer in China, hepatocellular carcinoma (HCC) could be divided into three types: hepatocellular carcinoma, bile duct cell carcinoma, and mixed carcinoma.[1,2] The main causes of HCC are chronic active hepatitis, including viral hepatitis caused by hepatitis B virus (HBV) and hepatitis C virus (HCV). Besides, the following factors were also confirmed highly associated with the occurrence of HCC including alcoholic hepatitis and non-alcoholic steatohepatitis.[3] Compared with other solid tumors, early detection of liver cancer is more difficult. At the time of diagnosis of primary liver cancer, more than 90% of patients are in the middle or advanced stage.[4] Surgical treatment for early diagnosis of subclinical liver cancer or small liver cancer has a good effect, and in the middle and advanced liver cancer, patients can be operated on only 5%-10% of the patients with liver cancer.[5,6] Even for early hepatocellular carcinoma or small hepatocellular carcinoma, surgical resection cannot solve the problem of intrahepatic recurrence or removal of multi-center lesions. Therefore, while strengthening the research on the early detection rate of liver cancer, how to enhance the efficacy of liver cancer, prevent its recurrence and metastasis, and develop a new approach to assist or even replace surgical treatment has become a hot spot in liver cancer research.

Current study revealed that, by using the TCGA (Cancer Genome Atlas) database to analyze data from about 3000 cases of nine types of cancer. It was found that AHNAK (neuroblast differentiation-associated protein) is one of the potential new oncogenes and a clinical diagnostic indicator.[7,8] Recent evidence suggested that AHNAK was highly associated with metastasis of HCC. In brief, AHNAK could induce the pseudopodia formation, which was the essential condition for cell migration and invasion.[9] Other recent studies also revealed that AHNAK may be involved in the induction and transformation of epithelial cells of colon, leading to epithelial oncogenesis, indicating that AHNAK played a crucial role in the development of HCC.[10]

Circular RNAs (circRNAs) were a subtype of new identified RNAs with the characteristics of circular structure.[11] Some circRNAs were identified with protein-coding ability.[12,13] Increasing evidence revealed that circRNAs was participated in multiple human disease including malignant cancer through different pathways.[14] In brief, circRNAs have been extensively involved in cell proliferation, apoptosis, cell invasion, and self-metabolic reprogramming during the occurrence or development of cancer. By forming the ceRNA loops, circRNAs could direct binding with specific miRNAs and act as sponges to regulate target genes to perform their function.[15,16]

In this study, we aimed to explore the potential circRNA interacting with AHNAK and further investigate the potential function of circRNA during the hepatocarcinogenesis process. Additionally, we also focused on the detailed mechanism regarding whether the aberrant expression of AHNAK was associated with circRNA as well as the detailed regulation mechanism.

TABLE 1 Clinicopathological relevance analysis of circRNA expression in clinical samples

Feature	circ_008194		
	Low	High	p value
All cases	20	20	
Age			
<60	10	9	0.752
≥60	10	11	
Gender			
Male	18	17	0.633
Female	2	3	
Differentiation grade			
Well	9	10	0.675
Moderate	7	8	
Poorly	4	2	
Tumor Size (cm)			
≤3 cm	17	18	0.633
>3 cm	3	2	
Metastasis			
Positive	15	6	**0.004**
Negative	5	14	
TNM stage(I:II:III)	10:8:2	9:8:3	0.881

Note: Data were analyzed by chi-squared test. *p* value in bold indicated statistically significant.

2 | MATERIALS AND METHODS

2.1 | Patient samples

From 2014 to 2020, 40 paired HCC cancer and matched normal tissues from patients who had undergone radical resection of HCC in the Second Affiliated Hospital of Nanjing Medical University were obtained and fixed in formalin at once. All clinical and pathological diagnosis were confirmed by two pathologists, according to the 8th edition of the AJCC and UICC. The research was approved by the ethics committee of the Second Affiliated Hospital with Nanjing Medical University, and all patients signed an informed consent form. All the procedures were carried out in compliance with government policy and the Declaration of Helsinki. All patients provided written informed consent to participate in this study. The relevant information of all patients was collected and presented in Table 1. All cell lines in this study were identified and analyzed by STR.

2.2 | RNA extraction and quantitative real-time polymerase reaction (qRT-PCR)

TRIzol Reagent (Takara) was used to isolate complete RNA from HCC tissues, normal tissues, and cell lines, and genomic DNA (gDNA) was extracted using FastPure DNA Isolation (Vazyme). Nanodrop 2000 was

used to examine the concentration and purity of RNA samples (Thermo Fisher Scientific). Reverse transcriptions of circRNA and mRNA were carried out with the PrimeScript RT Master Mix (Takara) and designed primers, with GAPDH as an internal control. Reverse transcriptions for miRNA were carried out with the Bulge-LoopTM miRNA qRT-PCR Starter Kit (RIBOBIO) and unique stem-loop primers, with U6 acting as an internal control, and cDNA amplification was achieved with an ABI Prism 7900 sequence detection system and TB Green Premix Ex Taq II (Takara; Applied Biosystems). Each sample was obtained three times. To compare relative quantification of circRNA, miRNA, and mRNA expression to an internal regulation, the $2^{-\Delta\Delta CT}$ method was used. The primer for GAPDH was Forward 5′- GGAGCGAGATCCCTCCAAAAT-3′; Reverse: 5′- GGCTGTTGTCATACTTCTCATGG-3′, for circ-0008194, Forward 5′- CTCGTCGCCGCCAGTAG -3′; and Reverse: 5′- TCTTTGCAGGATTCCGCTCA -3′.

2.3 | Cell counting kit-8 proliferation assay

In each well of a 96-well plate, 1000 cells were plated in total. The CCK-8 reagent (Dojindo Seed) was added directly to the culture medium at the stated time (24, 48, 72, and 96 h). Cells were then incubated at 37°C for 2 h, and the optional density (OD) value was measured at 450 nm by microplate reader (BioTek Instruments). These studies were carried out three times.

2.4 | Transwell assay

Cells were seeded in upper chambers with 200ul of serum-free medium for Transwell assays. The transwell chamber (Corning) was paved with matrigel mix (BD Biosciences) for invasion assays. The bottom chamber medium contained 10% FBS to attract upper cells. The upper chambers were set and stained for 20 min with a 0.5% crystal violet solution after a 48-h incubation period. The cell lines were photographed and counted in five distinct regions. In total, five independent visual fields were randomly selected for imaging, and ImageJ was used for optical density analysis.

2.5 | RNA immunoprecipitation assay

The RNA immunoprecipitation (RIP) assay was carried out according to the manufacturer's instructions using the Magna RIP™ RNA-binding protein immunoprecipitation kit (Millipore). In brief, cells were lysed in RIP lysis buffer and the cell lysates were incubated with RIP buffer containing magnetic beads conjugated with human anti-Argonaute2 (AGO2) antibody (Millipore) or negative control mouse IgG (Millipore). The magnetic beads coated with antibodies were added to the extracted RNA suspension and incubated on ice for 30 min. After eluting the magnetic beads, we extracted the RNA and purified by using the purification kit. Then, PCR was used for quantitative analysis.

2.6 | RNA pull-down assay

The biotin-coupled circ_0008194 probe and control oligo probe were designed and synthesized by RiboBio (Guangzhou). Briefly, cells were lysed with lysis buffer and 50 μl of the cell lysates were aliquot for input. After incubated with the biotin-coupled probe at room temperature for 1 h, the rest were incubated with streptavidin magnetic beads (Life Technologies) at 4°C for 4 h to capture the probe-RNA complexes. Then, the beads were washed with lysis buffer. Finally, RNAs bound to the beads were isolated with TRIzol Reagent (Invitrogen) and analyzed by qRT-PCR.

2.7 | Luciferase reporter assay

The circRNA and AHNAK–3′UTR sequences, as well as their corresponding mutations, were designed, synthesized, and inserted into the luciferase reporter vector pmiR-RB-Report vector (RIBOBIO). The plasmid was transfected into cells via Lipofectamine™ 2000. After 48 h, firefly or Renilla luciferase assay reagent was mixed with cell lysate in each group. Luciferase Reporter Gene Assay kit (GM-040501A, Genomeditech) was adopted for assessing luciferase activity on an Infinite M1000 PRO microplate reader (Tecan Group, Ltd.).

2.8 | Statistical analysis

SPSS 20.0 (IBM, SPSS) and GraphPad Prism 5 were used for statistical analysis. To explore whether two or more classes were statistically significant, we used the Student t-test and one-way ANOVA. The relationships were examined using the Pearson correlation coefficient. The data were interpreted as a mean standard deviation. For analyzing the difference between the two groups, we employed the Student t-text based on the homogeneity of variance. For comparing difference in multiple groups (>2), the ANOVA Kruskal–Wallis test was used. For all studies, $p < 0.05$ between groups were considered statistically significant.

3 | RESULTS

3.1 | Circ_0008194 interact with AHNAK in HCC

Since AHNAK has been identified highly associated with tumor metastasis, we firstly investigated the endogenous level of AHNAK in tissues samples of HCC patients. As presented in Figure 1A, we confirmed the upregulation of AHNAK in tumor tissues of HCC. We also revealed an increased protein level of AHNAK in tumor tissues (Figure 1B). According to the circRNA database (https://circinteractome.nia.nih.gov/circular_rna.html), the hsa_circ_0008194 was spliced from the DNA sequence of AHNAK. The relative expression of circ_0008194 in the tissue's samples used above was
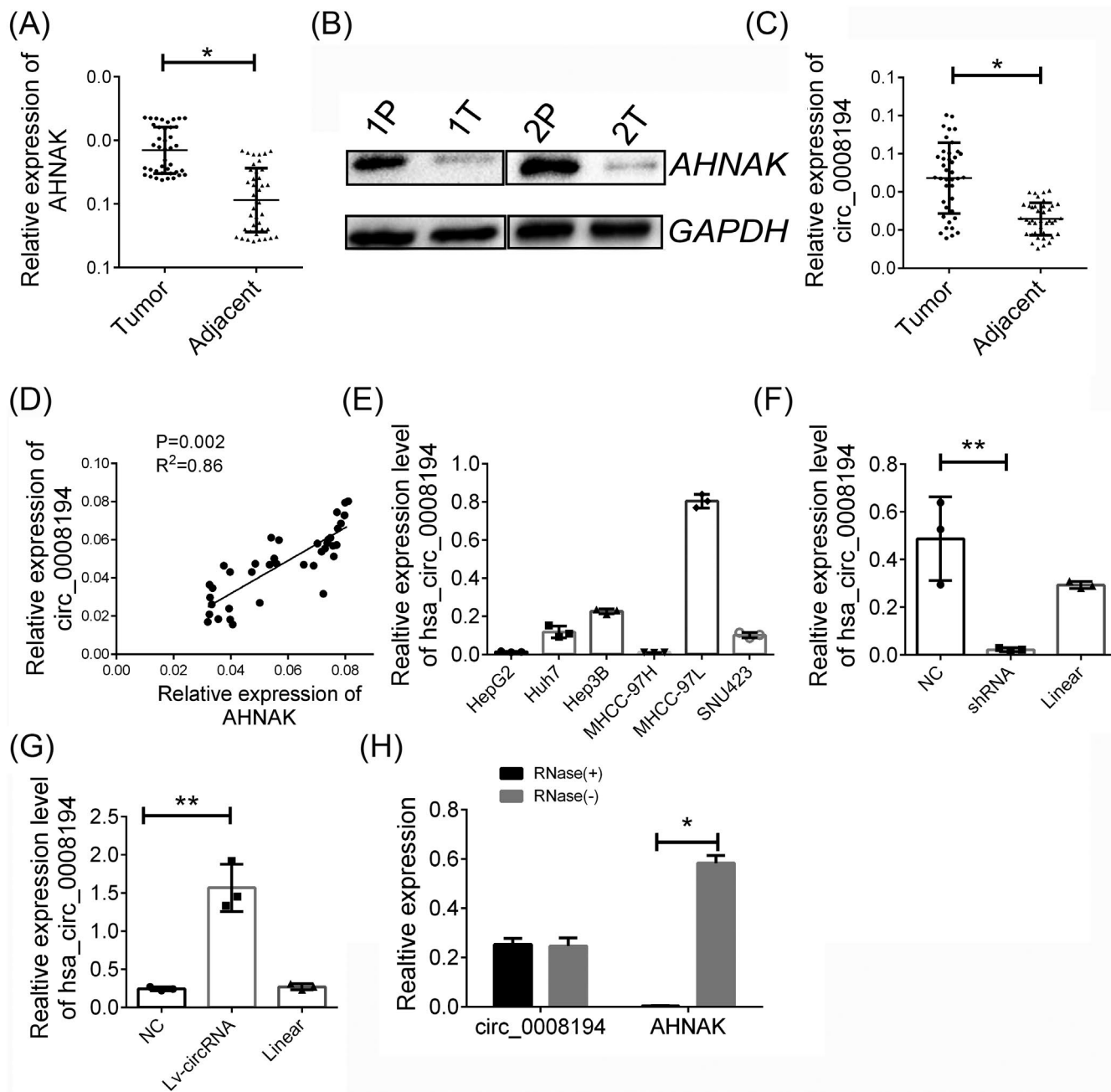
FIGURE 1 AHNAK and circ_0008194 was expressed at high levels in HCC tissues and cell lines. (A) QRT-PCR was used to detect relative expression of AHNAK in HCC tissues and matched para-cancer tissues ($n = 40$). (B) Protein expression level of AHNAK protein in HCC tissues. (C) QRT-PCR was used to detect relative expression of circ_0008194 in HCC tissues and matched para-cancer tissues. (D) Correlation analysis of AHNAK and circ_0008194. (E) RT-PCR confirmed the expression of circ_0008194 in cell lines. (F) Hep3B cells treated with circ_0008194 shRNA. (G) Hep3B cells treated with circ_0008194 overexpressed lentivirus. (H) Cells treated with RNase and detected by PCR (n.s indicated no significance, $^*p < 0.05$, $^{**}p < 0.001$)

also examined. As presented in Figure 1C, the upregulated level of circRNA was also obtained. Further Pearson correlation analysis identified a positive correlation between circ_0008194 and AHNAK ($p = 0.002$, $R^2 = 0.86$, Figure 1D). The clinical characteristics analysis for circ_0008194 indicated that circ_0008194 was corrected with the metastasis of HCC (Table 1).

We further tested the regulation of circ_0008194 on cell biological behavior by knockdown and overexpression. In order to

detect the contact of endogenous expression in cells, we selected Hep3B as the cell model with moderate expression-related abundance (Figure 1E). Cells were treated with circ_0008194 shRNA lentivirus and the overexpressing lentivirus vector. The knockdown was confirmed targeting circ_0008194 instead of the linear pattern (Figure 1F). We further confirmed that circ_0008194 was overexpressed by RT-PCR (Figure 1G). Since the function of circ_0008194 is still unknown at present, we further treated the above samples

with RNase and identified whether the circ_0008194 was in circular structure. The results showed that the expression of circ_0008194 did not altered after RNase treatment (Figure 1H).
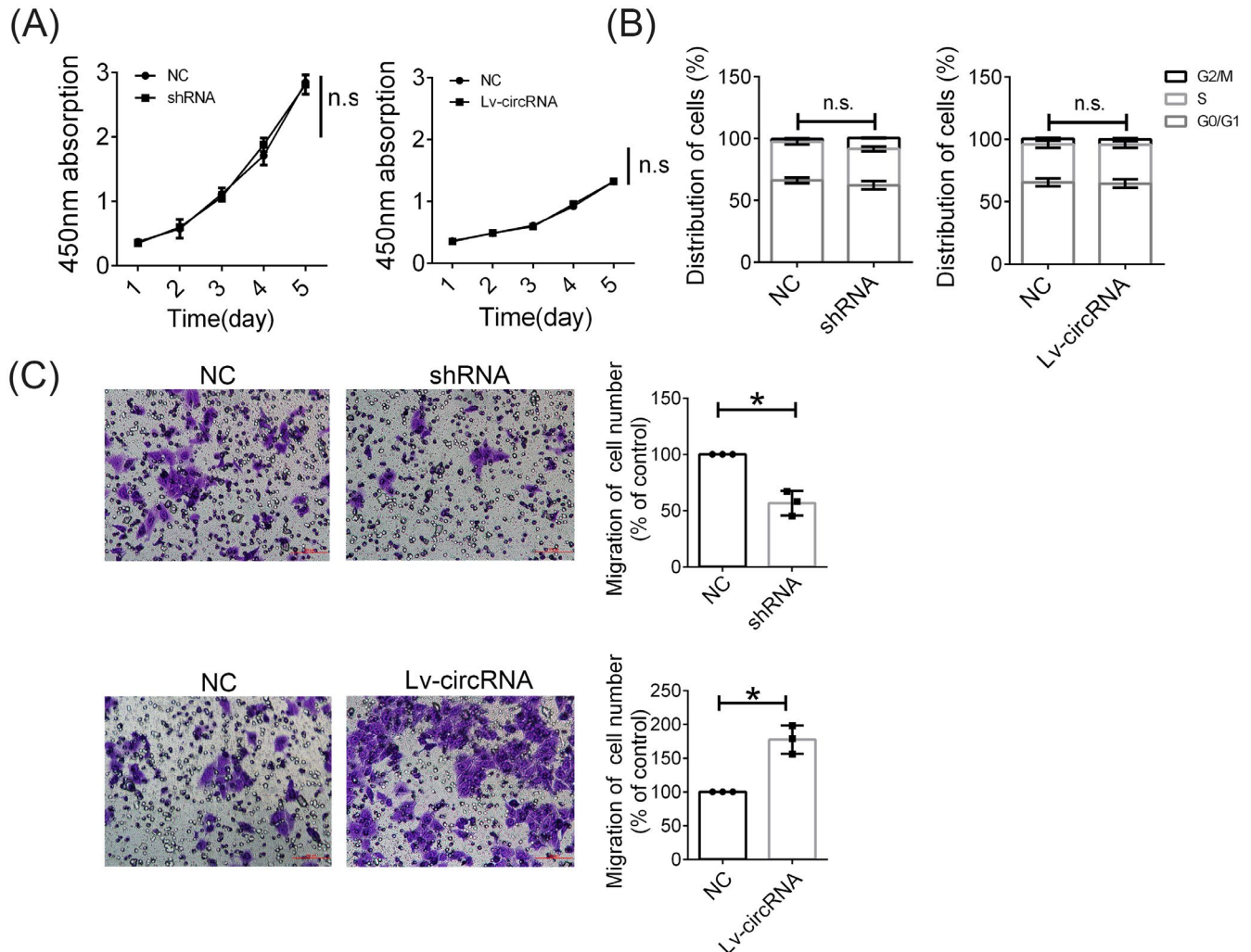
3.2 | Circ_0008194 promoted cell invasion in vitro

The aberrant expression of circ_0008194 in HCC patients indicated a high association with tumor metastasis; to further explore the function of circ_0008194 in the development of HCC, we first investigated the cell proliferation by treating cells with either shRNA or overexpression lentivirus. As presented in Figure 2A, CCK-8 assay indicated that knocking down or increasing the level of circ_0008194 could not alter the growth of HCC cells. Besides, the cell cycle distribution detected by flow cytometry also reveals no difference with the loss or ectopic expression of circ_0008194 (Figure 2B). The transwell assay was used to examine function of circRNA in cell invasion. Interestingly, the migrated cells were decreased when Hep3B

was treated with circ_0008194 shRNA lentivirus while could be increased with overexpressing of circ_0008194 (Figure 2C). These results were consistent with the oncogenic function of circ_0008194 during the development of HCC.
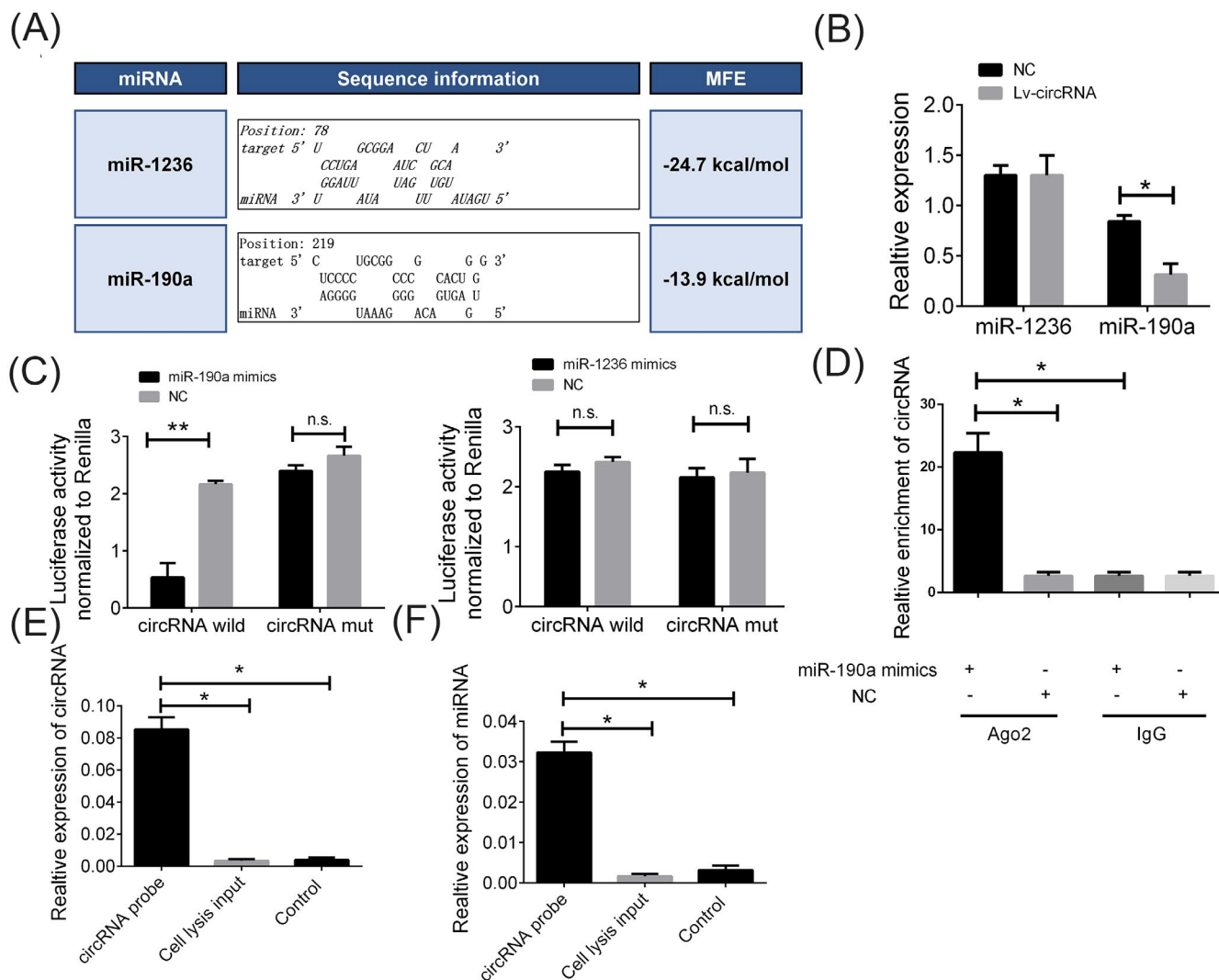
3.3 | Circ_0008194 could be bound with miR-190a

circRNAs were identified as a sponge to interact with certain miRNA and target genes through a ceRNA approach. Thus, the bioinformatical analysis was applied to predict the potential miRNA, which might bind with circ_0009184. As presented in Figure 3A, two miRNAs including miR-1236 and miR-190a were obtained with potential binding site. The expression of the two miRNAs was further detected in cells; we found a significant suppression of miR-190a by overexpression of circ_0008194. However, no difference was found in miR-1236 (Figure 3B). We also employed the luciferase reporter assay to detect whether there were potential regions binding to miR-190a in

FIGURE 2 circ_0008194 promoted cell invasion in vitro. (A) To evaluate the ability of proliferation in cells transfected with circ_0008194 knocking-down and overexpression lentivirus, CCK-8 assays were used. (B) The distribution of cell cycle stage was detected by flow cytometry. (C) Transwell assay was used to evaluate cell invasive capabilities in HCC cells. (n.s indicated no significance, $*p < 0.05$, $**p < 0.001$)

FIGURE 3 circ_0008194 could be directly bound by miR-190a. (A) The detailed binding site between miRNA and circ_0008194. (B) miRNA expression level in cells. (C) The relative luciferase activities were detected in cells after co-transfection with circRNA and miRNA, respectively. Data are all represented as mean $\pm$ SD ($n = 3$). (D) Anti-Ago2 RIP assay was executed in cells after transfection followed by qRT-PCR to detect circ_0008194. (E, F): Biotinylated circ_0008194 probe and a NC probe were used to pull down the candidate miRNAs and tested with quantitative real-time PCR (n.s indicated no significance, *$p < 0.05$, **$p < 0.01$)

circRNA sequences. The wild type and the specific mutant type targeting the prediction binding site were synthesized. As presented in Figure 3C, the luciferase intensity was decreased when treating cells with miR-190a to cells overexpressed with wild AHNAK. No difference was obtained in the rest of the groups. RIP results also showed that more circ_0008194 could be captured by AGO2 antibody in miR-190a overexpressed cells (Figure 3D). We also employed the pull-down assay to investigate whether circ_0008194 direct bind with miR-190a. The biotin-labelled circ_0008194 probe was used. Following investigation also reveals that miR-190a was detectable in HCC cells treated with circ_0008194 probe (Figure 3E, F).

3.4 | AHNAK was the potential target of miR-190a

In order to clarify in detail how circ_0008194 interacted with miR-190a and whether miR-190a was involved in the dysregulated

expression of AHNAK, we detected the expression of miR-190a in HCC tissues. The decreased level of miR-190a was confirmed in tumor tissues (Figure 4A). Pearson correlation analysis confirmed this finding. We found circ_0008194 was reversely correlated with miR-190a, and miR-190a was reversely correlated with AHNAK (Figure 4B). Bioinformatical analysis also revealed a detailed binding site between miR-190a and AHNAK (Figure 4C). By constructing wild-type and mutated plasmids of AHNAK 3′UTR, we confirmed the presence of miR-190a binding site in 3′UTR region of AHNAK by using dual-luciferase reporter gene assay (Figure 4D). Furthermore, miR-190a overexpression or circ_0008194 knocking-down was performed in cell lines respectively to explore the interaction. The results showed that either miR-190a overexpression or circ_0008194 knocking-down could inhibit AHNAK expression. In addition, artificially increasing the expression of circ_0008194 also promoted the expression of AHNAK (Figure 4E). We also investigated the protein expression
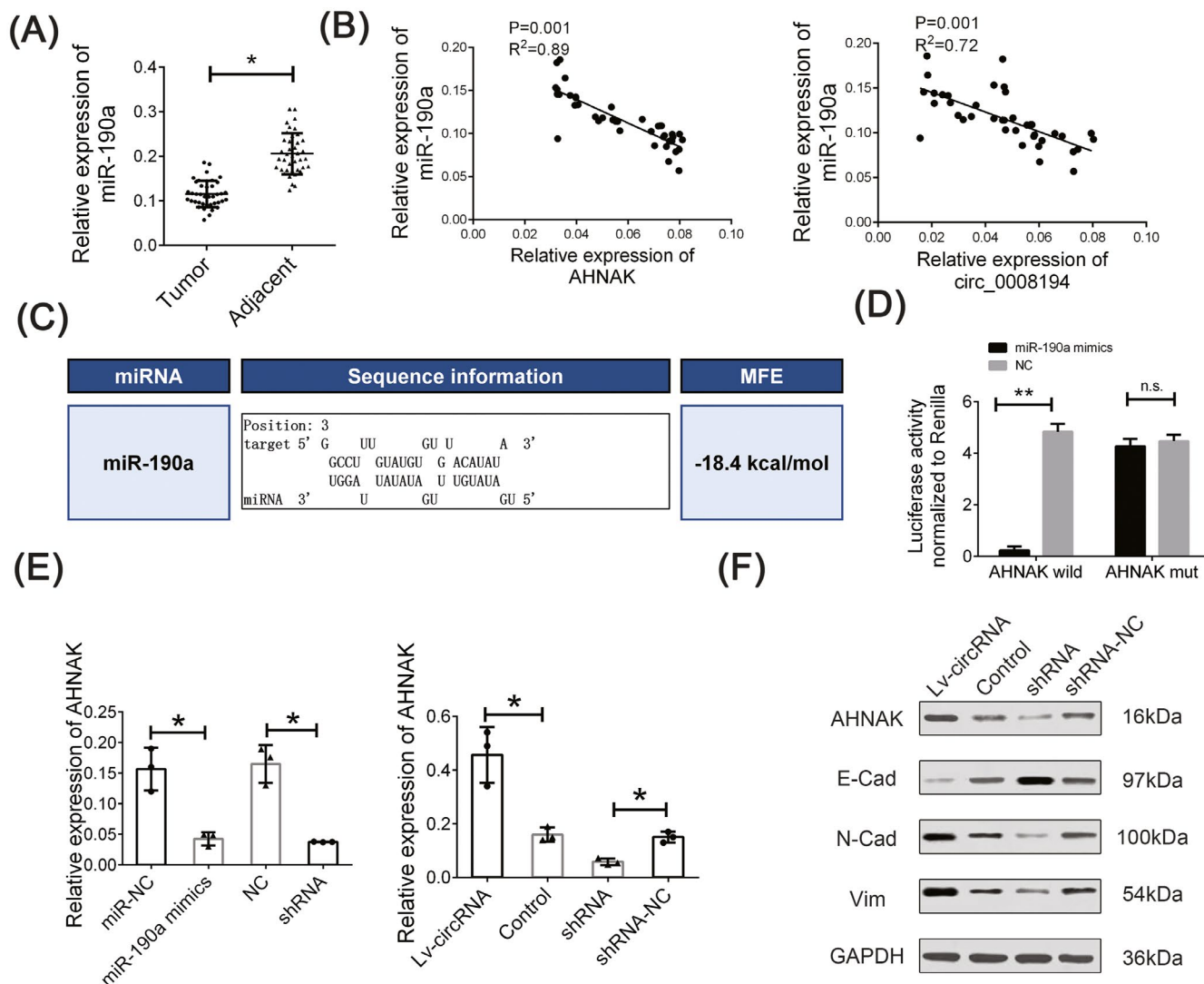
FIGURE 4 miR-190a could reversely regulated AHNAK through 3'UTR region binding. (A) QRT-PCR was used to detect relative expression of miR-190a in HCC tissues and matched para-cancer tissues ($n = 40$; $n = 40$). (B) Pearson correlation analysis between miR-190a/AHNAK and miR-190a/circ_0008194. (C) The detailed sequence for miR-190a bound to AHNAK. (D) Dual-luciferase reporter assay. (E) Relative expression of AHNAK in miRNA mimics and circRNA shRNA-treated cells and relative expression of AHNAK in cells treated with circRNA overexpression and shRNA lentivirus. (F): Relative protein expression level of AHNAK and metastasis markers in cells treated with circRNA overexpression and shRNA lentivirus (n.s indicated no significance, *$p < 0.05$, **$p < 0.01$)

level of ANHAK in cells treated with circRNA_0008194 overexpression lentivirus. As presented in revised Figure 4, we found that the protein level of ANHAK was increased with the overexpression of circRNA_0008194. The tumor metastasis markers were also examined. We found the epithelial marker E-cadherin was decreased by circRNA_0008194, while the stromal cell markers such as N-cadherin and Vimentin were increased. We also found the opposite result in the knockdown cells (Figure 4F), indicating the circRNA_0008194, was highly associated with tumor metastasis.

4 | DISCUSSION

AHNAK is a nuclear protein of about 700 kDa weight, which is widely expressed in various cells.[17] Due to its complex structure,

it may have a special function or function as a scaffolding protein. Earlier studies suggested that AHNAK was mainly localized in the nucleus and contained potential nuclear localization sequence (NLS) in the carboxy-terminal domain of AHNAK protein.[18] Subcellular location indicated AHNAK is localized mainly in cytoplasm and/or associated with the cell membrane.[19] A possible explanation for the difference in AHNAK protein localization is AHNAK's ability to shuttle between various subcellular components. For example, in keratinocytes, AHNAK can be translocated from the cytoplasm to the cell membrane in a manner dependent on calcium ions and protein kinase C. In addition, AHNAK contains a nuclear output signal (NES) sequence that allows AHNAK to be transported from the nucleus following intercellular contact in epithelial cells and activation of protein kinase B.[20] The detailed molecular function of AHNAK still needs to be further investigated.

As reported, AHNAK is involved in various biological processes, including blood-brain barrier formation, cell structure formation, cell migration, cardiac calcium channels regulation, and the reparation of muscle.[21] In addition, recent evidence suggests that AHNAK may be involved in promoting tumor metastasis. AHNAK was also confirmed highly associated with tumor metastasis by regulating cell invasion; in addition, AHNAK is closely related to pseudopod formation.[22] High expression of AHNAK in tumor tissue suggests a poor prognosis. In addition, inhibition of the expression of AHNAK could significantly reduce the ability of cells to metastasize.[23] Previous studies have shown that a specific gene may have different functions in different tumors. In this study, AHNAK plays the role of a tumor suppressor gene in reproductive system tumors, but there are many reports on its carcinogenic effect in digestive tract tumors, which is consistent with the findings of this study. This may be related to the origin of tumor cells and the specific expression of specific genes in different tumor cells.

circRNAs are relatively stable RNAs formed by a special mechanism of ring formation and widely exist in eukaryotic cells. circRNAs play important roles in many pathophysiological processes, including the genesis and development of tumors. It was well proved that circRNA was involved in the genesis, development and prognosis of primary hepatocellular carcinoma. For the ceRNA mechanism, multiple circRNAs have been proved to interacting with miRNA and protein-coding RNA in human cancers. For example, suppression of CirchipK2 was reported to inhibit the DDP resistance in ovarian cancer (OVC) through regulating CHTOP as a ceRNA approach.[24] In addition, circ_0032822 could promote the prognosis of laryngeal cancer through the miR-141/E2F3 axis.[25] Previously, research also showed that increased miR-190a could suppress the expression of PAR1 and induced the inhibition of cell migration and invasion in breast cancer. This result was consistent with our finding that miR-190a might be a tumor suppressor gene.[26] Besides, the tumor suppressor function of miR-190a was also confirmed in the development of HCC. They found that ectopic expression of miR-190a in HCC cells could decrease the invasion of cells.[27]

In summary, we explored the function of circ_0008194 as an oncogenic gene in the development of HCC. In addition, circ_0008194 can promote the progression of liver cancer by acting as a sponge and mediating the formation of the ceRNA loop by miR-190a and AHNAK. These results provide theoretical basis for the research and development of targeted therapeutic targets for liver cancer in the future.

CONFLICT OF INTEREST

No potential conflict of interest was reported by the authors.

AUTHOR CONTRIBUTIONS

GJZ involved in conceived and designed the experiments. WL, YP, and HBZ performed the experiments. YZ and HZ analyzed the data. LL and QL contributed reagents/materials/analysis tools. All authors contributed to the article and approved the submitted version.

CONSENT FOR PUBLICATION

Written informed consent for publication was obtained from all participants.

DATA AVAILABILITY STATEMENT

The datasets used and/or analyzed during the current study are available from the corresponding author on reasonable request.

ORCID

Guozhong Ji https://orcid.org/0000-0002-2098-0689

REFERENCES

1. Tang J, Zhuo H, Zhang X, et al. A novel biomarker Linc00974 interacting with KRT19 promotes proliferation and metastasis in hepatocellular carcinoma. *Cell Death Dis.* 2014;5:e1549.
2. Zucman-Rossi J, Villanueva A, Nault JC, Llovet JM. Genetic landscape and biomarkers of hepatocellular carcinoma. *Gastroenterology.* 2015;149(5):1226-1239.e1224.
3. Zhu M, Zheng J, Wu F, et al. OPN is a promising serological biomarker for hepatocellular carcinoma diagnosis. *J Med Virol.* 2020;92(12):3596-3603.
4. Yong KJ, Gao C, Lim JS, et al. Oncofetal gene SALL4 in aggressive hepatocellular carcinoma. *N Engl J Med.* 2013;368(24):2266-2276.
5. Farazi PA, DePinho RA. Hepatocellular carcinoma pathogenesis: from genes to environment. *Nat Rev Cancer.* 2006;6(9):674-687.
6. Llovet JM, Montal R, Sia D, Finn RS. Molecular therapies and precision medicine for hepatocellular carcinoma. *Nat Rev Clin Oncol.* 2018;15(10):599-616.
7. Li Y, Lv X, Chen H, et al. Peptide derived from AHNAK inhibits cell migration and proliferation in Hirschsprung's disease by targeting the ERK1/2 pathway. *J Proteome Res.* 2021;20(5):2308-2318.
8. Cho WC, Jang JE, Kim KH, Yoo BC, Ku JL. SORBS1 serves a metastatic role via suppression of AHNAK in colorectal cancer cell lines. *Int J Oncol.* 2020;56(5):1140-1151.
9. Sohn M, Shin S, Yoo JY, Goh Y, Lee IH, Bae YS. Ahnak promotes tumor metastasis through transforming growth factor-beta-mediated epithelial-mesenchymal transition. *Sci Rep.* 2018;8(1):14379.
10. Sudo H, Tsuji AB, Sugyo A, Abe M, Hino O, Saga T. AHNAK is highly expressed and plays a key role in cell migration and invasion in mesothelioma. *Int J Oncol.* 2014;44(2):530-538.
11. Wang R, Zhang S, Chen X, et al. CircNT5E acts as a sponge of miR-422a to promote glioblastoma tumorigenesis. *Can Res.* 2018;78(17):4812-4825.
12. Lu Y, Li Z, Lin C, Zhang J, Shen Z. Translation role of circRNAs in cancers. *J Clin Lab Anal.* 2021;35(7):e23866.
13. Zhao W, Zhang Y, Zhu Y. Circular RNA circbeta-catenin aggravates the malignant phenotype of non-small-cell lung cancer via encoding a peptide. *J Clin Lab Anal.* 2021;35(9):e23900.
14. Kristensen LS, Andersen MS, Stagsted LVW, Ebbesen KK, Hansen TB, Kjems J. The biogenesis, biology and characterization of circular RNAs. *Nat Rev Genet.* 2019;20(11):675-691.
15. Chen LL. The biogenesis and emerging roles of circular RNAs. *Nat Rev Mol Cell Biol.* 2016;17(4):205-211.

16. Memczak S, Jens M, Elefsinioti A, et al. Circular RNAs are a large class of animal RNAs with regulatory potency. *Nature*. 2013;495(7441):333-338.

17. Ghodke I, Remisova M, Furst A, et al. AHNAK controls 53BP1-mediated p53 response by restraining 53BP1 oligomerization and phase separation. *Mol Cell*. 2021;81(12):2596-2610.

18. Kim YN, Shin JH, Kyeong DS, et al. Ahnak deficiency attenuates high-fat diet-induced fatty liver in mice through FGF21 induction. *Exp Mol Med*. 2021;53(3):468-482.

19. Zhang S, Lu Y, Qi L, Wang H, Wang Z, Cai Z. AHNAK2 Is associated with poor prognosis and cell migration in lung adenocarcinoma. *Biomed Res Int*. 2020;2020:8571932.

20. Cimas FJ, Manzano A, Baliu-Pique M, et al. Genomic mapping identifies mutations in RYR2 and AHNAK as associated with favorable outcome in basal-like breast tumors expressing PD1/PD-L1. *Cancers*. 2020;12(8):2243.

21. Davis TA, Loos B, Engelbrecht AM. AHNAK: the giant jack of all trades. *Cell Signal*. 2014;26(12):2683-2693.

22. Shafran JS, Andrieu GP, Gyorffy B, Denis GV. BRD4 regulates metastatic potential of castration-resistant prostate cancer through AHNAK. *Mol Cancer Res*. 2019;17(8):1627-1638.

23. Peng R, Zhang PF, Yang X, et al. Overexpression of RNF38 facilitates TGF-beta signaling by Ubiquitinating and degrading AHNAK in hepatocellular carcinoma. *J Exp Clin Cancer Res*. 2019;38(1):113.

24. Cao Y, Xie X, Li M, Gao Y. CircHIPK2 contributes to DDP resistance and malignant behaviors of DDP-resistant ovarian cancer cells both in vitro and in vivo through circHIPK2/miR-338-3p/CHTOP ceRNA pathway. *Onco Targets Ther*. 2021;14:3151-3165.

25. Zhang S, Han J, Fu J. The circ_0032822 promotes the proliferation of head and neck squamous cell carcinoma cells through miR-141/EF3 signaling axis. *Front Oncol*. 2021;11:662496.

26. Chu HW, Cheng CW, Chou WC, et al. A novel estrogen receptor-microRNA 190a-PAR-1-pathway regulates breast cancer progression, a finding initially suggested by genome-wide analysis of loci associated with lymph-node metastasis. *Hum Mol Genet*. 2014;23(2):355-367.

27. Wang X, Ren Y, Yang X, et al. miR-190a inhibits epithelial-mesenchymal transition of hepatoma cells via targeting the long non-coding RNA treRNA. *FEBS Lett*. 2015;589(24 Pt B):4079-4087.